ELSEVIER

PII: S0308-8146(96)00019-2

Food Chemistry, Vol. 56, No. 3, pp. 231–240, 1996

0308-8146/96 $15.00+.00

Computer modelling studies of the water-structuring properties of carbohydrates and the sweetness response

Tim Astley,[a] Gordon G. Birch,[b] Michael G. B. Drew,[a]* P. Mark Rodger[a] & Gareth R. H. Wilden[a]

[a]Department of Chemistry, [b]Department of Food Science and Technology, The University of Reading, Whiteknights, Reading RG6 2AD, UK

(Received 29 August 1995; revised version received 11 December 1995; accepted 19 December 1995)

Molecular dynamics calculations have been carried out for a variety of carbohydrates in aqueous solvent to ascertain their water-structuring capabilities. Radial distribution functions have been calculated for oxygen, carbon and hydrogen atoms in a range of different environments. These functions are able to reveal quite different and distinctive behaviour of the solvent around the atom types and in particular can distinguish between hydrophilic and hydrophobic hydration effects. The arrangements of water molecules around the different hydroxide groups in the sweet tasting α-D-mannopyranose and the bitter tasting anomer β-D-mannopyranose have been calculated and the radial distribution functions show significant differences between hydroxyl groups in the same molecule and the equivalent hydroxyl groups in different molecules. Methods are assessed for the summation of hydrogen bonds around the carbohydrate oxygen atoms. The results of the molecular dynamics calculations are consistent with previous experimental and theoretical data about the taste properties of these two molecules. Copyright © 1996 Elsevier Science Ltd

INTRODUCTION

The involvement of hydrogen bonding in sweetness was first hypothesized for sugars by Shallenberger (1963). Not long after a correlation was found by Shallenberger & Acree (1967) between sweet taste and different compounds regardless of their chemical class, depending on the existence of an AH–B system capable of establishing two hydrogen bonds with a corresponding B–AH unit on the receptor. There was a distance constraint between the donor and acceptor proton of 2.5 to 4.0 Å. This system was extended by Kier (1972) who added a dispersion site (X) generally designated as a hydrophobic centre γ. The γ centre seems to be essential in defining the quality of taste in high potency sweeteners. This three-centre model was further refined by van der Heijden *et al.* (1985) who introduced the parameters α, δ and ω, indicating the existence of a minimum, an optimum and a maximum distance between the hydrophobic centre and the hydrophilic AH–B moiety in a homologous series of sweeteners. Other attempts to improve the model have included adding barriers at varying distances from existing sites (Shallenberger *et al.*, 1969; Pautet & Nofre, 1978). Although this three body tenet is useful as a working hypothesis for structure–activity relationships and molecular modelling studies, it is far from being applicable to all sweet compounds and there have been many attempts to add more sites, culminating in the eight-sited model of Tinti & Nofre (1990).

One assumption that underlies these models is that it is the conformation of the sugar that is important and, as a consequence, water is not considered explicitly as one of the partners in sweet taste chemoreception. Therefore much work has been done on obtaining minimum energy structures and fitting specific sets of atoms to these *n*-sited models. These calculations were originally performed *in vacuo*, although, more recently, solvent effects have been included, either by including water molecules in the simulation (Brady, 1989; Ha *et al.*, 1991; Madsen *et al.*, 1990), or through the use of effective intramolecular potentials using 'extended atoms' (Grootenhuis & Haasnoot, 1993). However, as most workers accept that hydrogen bonding is the cornerstone of the sweetness mechanism it is difficult to justify ignoring the strongest H-bond acceptor/donor

*To whom correspondence should be addressed.

molecule, water, in any investigation of the mechanism. In line with the most recent ideas (Birch *et al.*, 1993), this paper focuses specifically on the behaviour and structure of water in the presence of a sugar, rather than on the behaviour of the sugar itself.

One experimental study which indicates the importance of water in taste response was carried out by Birch *et al.* (1993) and showed a strong correlation between apparent specific volumes (ASV) and taste class. The optimum specific volume for sweet taste was found to be between 0.51–0.71 $cm^3\ g^{-1}$. Sugars with a pure sweet taste lie in the middle of this range, while artificial sweeteners lie in the range 0.53–0.74 $cm^3\ g^{-1}$ in accord with their bitter aftertaste.

It is convenient to identify three classes of water/sweet molecule interaction. The first is the interaction in the solution bulk which affects the conformation adopted by the sweet molecule and mediates its long-range interaction with the receptor site. The second is the interaction as the sweet molecule is guided into the receptor site and the third is the interaction which holds the sweet molecule in place, thereby controlling the duration and intensity of the sweet taste response. To understand more fully the mechanism of sweet taste, a better understanding of all three classes of interaction between water molecules and the sweet taste molecule is required, including quantities such as the lifetime of hydrogen bonds, the packing of water molecules around certain sites on the sweet molecules and the mobility of water around the molecule.

In this paper we describe the initial results of a computer modelling study of the first class of sweet molecule/water interaction, i.e. the sweet molecule in bulk water solution. The molecular modelling calculations involved make use of numerical solutions of the equations that embody the physical laws that govern the system to predict its physical nature. At the most fundamental level, this approach would involve direct solution of Schrödinger's equation for the nuclear and electronic degrees of freedom, though such *ab initio* calculations are very computer-intensive and impossible in the practical sense for systems containing significant numbers of solvent molecules. The majority of calculations in solvent are therefore carried out using classical techniques such as molecular mechanics and molecular dynamics. Here, the Born–Oppenheimer approximation is invoked to focus on atomic coordinates and treat electrons only implicitly, thereby generating potential energy functions that describe the way in which the energy of the system changes with the positions of the constituent atoms. These energy functions are usually empirically derived, and consist of sums of terms representing various, identifiable contributions to the total energy of a molecule. For example, some terms represent the energy of stretching or compressing chemical bonds, bending bond angles, changing torsion angles, van der Waals (non-bonded) interactions and electrostatic interactions between the various partially charged atoms. The adjustable parameters that appear in these functions can then be selected by exhaustive comparison of calculated molecular properties with experimental measurements, in order to give the most physically realistic representation possible with the chosen functional form. There are several reputable but very different sets of parameters (force fields) that have been used and have been validated by the successful reproduction of experimental structures.

Although many of the interaction terms are well defined, the exact functional form needed to describe a hydrogen bond is still debated. Because of its relative strength compared with van der Waals interactions, being longer range, attenuating as $\sim r^{-1}$, and more angularly dependent, hydrogen bonding is often a powerful structuring force. This is certainly true for carbohydrates, which have hydroxyl groups that can simultaneously donate and accept hydrogen bonds. Rotatability of the hydroxyl groups and possible bifurcation make prediction of hydrogen bonding structures difficult, but the energy of hydrogen bonding is clearly a major force in determining carbohydrate structures. These considerations have led many workers to treat hydrogen bonds through explicit terms in the force field (e.g. an O–H...O angle bending term, or a special 10–12 Lennard–Jones potential) though these have now gone out of favour (Cieplak & Kollman, 1991) and most workers have recognized that the small size of a hydrogen-bonding proton makes it possible to reproduce H-bonding effects through a combination of atomic partial charges and van der Waals interactions.

Because of the effects of intermolecular hydrogen bonds, the study of isolated molecules may not be as helpful as desired for predicting conformations in condensed phases. Many studies of carbohydrates have been made by making the assumption that the conformation found in solution is the lowest energy conformation adopted by an isolated molecule; but carbohydrates are flexible with many different conformations that are separated by only a few kcal mol^{-1}, and the introduction of a few intermolecular hydrogen bonds can alter the relative energies of the conformations significantly. This has been confirmed through simulations that do include explicit solvent molecules.

An additional problem is that intramolecular hydrogen bonds are often found in crystal structures of the carbohydrates, thus suggesting that the lowest energy conformation should contain such bonds; however, it is well known that these intramolecular hydrogen bonds do not persist in solution, presumably because they are supplanted by hydrogen bonds with the solvent. Conformational search procedures for single molecules, therefore, need to reduce, artificially, the likelihood of intramolecular hydrogen bonds being formed if they are to predict the correct solution-phase structures (Grootenhuis & Haasnoot, 1993). These considerations are compounded by the effects of temperature. To interpret behaviour in terms of lowest energy conformations is to imply that the behaviour at absolute zero is a good model of the behaviour at room temperature; in reality there will be a great deal of conformational fluidity, particularly with respect to the

H-bond structure. Thus to assume that the lowest energy structure is representative of the whole system can be unrealistic. It is, then, a significant approximation to look for structural relationships between the lowest energy conformation of 'sweet' molecules, since both the flexibility of the molecules and the effects of the hydrogen-bonding solvent are ignored.

Many of these approximations have been motivated by technology: it is only recently that computer power has increased to the point that molecular modelling studies which treat the solvent explicitly are a realistic possibility. An additional benefit of this is that such modelling studies can also be used to examine the structure induced in the solvent by the sweet molecule, thereby elucidating possible mechanisms for water in the second class of sweet molecule/water interactions. One of the main aims of this work is to ascertain whether any pattern of solute–water interactions is common in sweet tasting molecules compared with non-sweet tasting molecules. Emergence of a correlation between some aspect of the solute–water interaction and taste quality would clearly be a substantial breakthrough. It must be stressed, however, that the nature of such solvation structure is still not well-established, and so many aspects of the local order generated by solute–water interactions still need to be investigated.

METHODOLOGY

Molecular dynamics (MD) simulations were used to model the behaviour of a dilute carbohydrate solution. The calculations were performed using the Quanta/CHARMm package (Quanta, 1994). The simulations involved one carbohydrate molecule surrounded by 278 water molecules contained within a cubic simulation box of sides 20 Å, and periodic boundary conditions were used to mimic the infinite solution. To test for effects of system size, some simulations were repeated with 125 or 491 water molecules (giving cubic simulation boxes of length 15 and 24 Å, respectively) but no significant differences were observed.

Calculations were carried out on α-D-mannopyranose and β-D-mannopyranose (Fig. 1) and the related compounds glucono-1,5-lactone, methyl-α-D-mannopyranoside and 1-methyl,1-deoxy-α-D-mannopyranose. The two D-mannopyranoses have different tastes, sweet and bitter, respectively, despite having very similar structures. The initial conformation of α-D-mannopyranose was taken from the crystal structure (Langchambon *et al.*, 1976); the initial conformation of β-D-mannopyranose was obtained from the crystal structure of the difluoro derivative (Withers *et al.*, 1986) and those of the other compounds were built from these structures. In view of the perceived lack of correlation between structures in the solid state and in solution, we then carried out a conformational search on the isolated molecules by using high temperature molecular dynamics in vacuum to generate a series of structures which were then minimized using molecular mechanics. It was

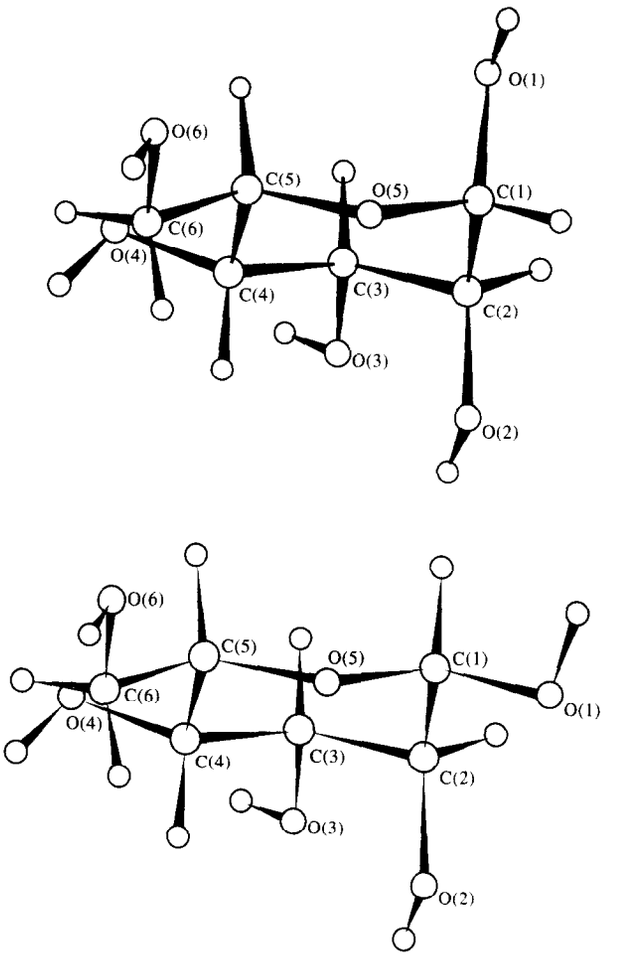

Fig. 1. The structures of α-D-mannopyranose and β-D-mannopyranose.

usually found that each carbohydrate had three or four local potential energy minima, and each of these was used in subsequent solvated simulations. Each structure was placed in the centre of a box of water molecules that had already been energy-minimized. Any water molecules with oxygen atoms whose van der Waals radii overlapped any of the atoms of the sugar were then deleted and the resulting structure again minimized to remove any 'hot-spots' caused by close contacts. Several different solute orientations were tried for the insertion process but the ensuing trajectories revealed no significant difference in any of the calculated quantities; this confirmed that our simulations were sampling the solvent equilibrium properly.

Intermolecular potentials for the carbohydrates were taken from the CHARMm force field. No explicit hydrogen bond function was employed (Brady, 1989). All hydrogen atoms were included explicitly in the simulations; that is 'united' or 'extended' atom representations were not used. The choice of a water force field is important but difficult to make because no model is accepted as ideal. The simplest and most commonly used are three-body potentials such as SPC (Berendsen *et al.*, 1981), SPC/E (Toukan & Rahman, 1985) and TIP3P (Jorgensen *et al.*, 1983). These associate all the repulsion/dispersion interactions with the oxygen atom,

while electrostatic interactions are modelled by three point charges coincident with the atomic positions. Four-body systems (e.g. TIP4P; Berendsen *et al.*, 1987) are also in use. The calculations reported in this work used TIP3P, which is the default in CHARMm; calculations employing the SPC/E and TIP4P potentials are in hand. All intermolecular potentials were modulated by a switching function so that the long-range interactions vanished smoothly for separations in the range 7.0–8.5 Å (Brooks *et al.*, 1983). In order to avoid artificially splitting molecular dipoles with this long range truncation, the switching was applied on a group-by-group rather than an atom-by-atom basis, with the groups corresponding to electrostatically neutral groups in the solute and to complete water molecules for the solvent. Equations of motion were integrated using the Verlet algorithm (Verlet, 1967) with a step size of 1 fs in most cases. The SHAKE algorithm (van Gunsteren & Berendsen, 1977) was used to ensure that all chemical bond lengths involving a hydrogen atom and all solvent bond angles remained constant throughout each simulation. The system was heated up from 0 to 300 K over 10 ps and then allowed to equilibrate for 10 ps. Following the equilibration period, the integration was continued without further interference for varying lengths of time, but typically several hundred picoseconds. In some cases the initial configuration prevented convergence of the SHAKE routine within a 1 fs timestep and so a smaller step size was used during the initial heating period in these systems. The trajectory files were analyzed using our own programs.

RESULTS AND DISCUSSION

The data obtained in the trajectory files have been used to calculate a series of functions that describe the water-structuring properties of the carbohydrates.

Radial distribution functions — generic effects

One of the more powerful methods of describing solvent structure is via the radial distribution function (rdf). These functions are able to reveal quite different and distinctive behaviour from different regions of the solvent, and in particular can distinguish between hydrophilic and hydrophobic hydration effects. The purpose of this section is to illustrate how different atoms within a carbohydrate give rise to different solvent behaviour; these general observations will then be used to characterize the differences between α-D-mannopyranose and β-D-mannopyranose.

The rdf is a measure of the average density of atoms or molecules found in a thin spherical shell of radius r centred on a specific atom or molecule. How this function depends on r, then, will depend on what atom or molecule is chosen as the centre of the shell, and what aspect of the surrounding medium is under consideration. Here we have concentrated on the distribution of solvent oxygen atoms about given solute atoms. To describe this we introduce the notation $g_{Ai}(r)$ to denote the distribution of water–oxygen atoms about atom A(i) from the solute; for example, $g_{O5}(r)$ refers to the distribution of solvent around the O(5) oxygen. The rdf is then rescaled by the bulk density so that a value above 1.0 indicates an above-average local density in that region. A comparison between the rdfs found in crystal structures and MD simulations has been given by van Eijck *et al.* (1990).

Figure 2 depicts rdfs for a number of different oxygen atoms found in α-D-mannopyranose and its related derivatives. The behaviour of these curves will be most easily understood by considering first the two extremes of behaviour. The rdf for the carbonyl oxygen in glucono-1,5-lactone, $g_{C=O}$ exhibits classic hydrophilic behaviour. There is a strong sharp peak at about 2.8 Å, which is the characteristic O–O separation in a hydrogen bond but would be very short for strictly non-bonding interactions; this is followed by a substantial depletion of solvent in the range 3.3–4.7 Å from O(1), followed by a secondary peak at about 5 Å. In pure water this secondary peak would be at about 4.5 Å, which is characteristic of the tetrahedral hydrogen bonding in such systems. For the purposes of comparison Fig. 2 also depicts the rdf g_{Me} for the methyl carbon in 1-methyl-1-deoxy-α-D-mannopyranose. This shows classic hydrophobic behaviour, with a broad first peak at about 3.8 Å corresponding to the first solvation shell, and no significant secondary structure.

The behaviour of atoms in mannopyranose can be seen to fall in between these two extremes. Both the ring hydroxyl oxygens which we have exemplified with g_{O1} and the CH_2OH group g_{O6} show hydrogen bonding behaviour. The O–O distance of *ca.* 2.9 Å is somewhat longer than in $g_{C=O}$, but is still short enough to imply strong hydrogen bonding effects. The first peak is

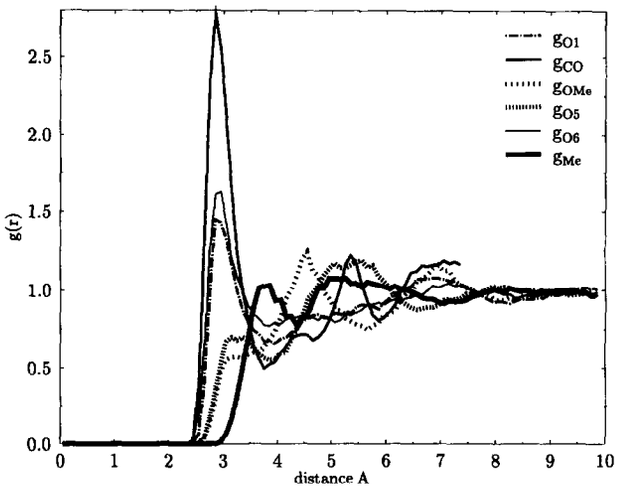

Fig. 2. Typical radial distribution curves $g(r)$ for an hydroxyl O(1), $g_{O1}(r)$; the unique O(6) in CH_2OH, $g_{O6}(r)$; the ethereal oxygen atom O(5), $g_{O5}(r)$, in α-D-mannopyranose; the carbonyl oxygen atom O(1) in glucono-1,5-lactone, $g_{C=O}(r)$; the methylated oxygen O(1) in methyl-α-D-mannopyranose, $g_{OMe}(r)$ and the carbon atom of the methyl group replacing the O(1)H moiety in 1-methyl-1-deoxy-α-D-mannopyranose, $g_{Me}(r)$; from dynamics runs on the appropriate compounds.

also lower for these mannopyranose oxygens. These differences between $g_{C=O}$ and g_{O1} are probably best understood in terms of packing effects: the glucono-1,5-lactone O(1) is more exposed to the solvent while both O(1) and O(6) in mannopyranose are partly obscured by the adjacent parts of the solute molecule, and have less space to accommodate hydrogen bonds to the solvent. The secondary structure is again present in g_{O1}, for mannopyranose, albeit much broader than for the $g_{C=O}$ in glucono-1,5-lactone. This secondary structure is absent, however, in g_{O6} for mannopyranose. Again, this is probably due to interference from the rest of the mannopyranose molecule, as the second solvation shell for O(6) will overlap the first solvation shell for O(5), the etheric oxygen.

The etheric oxygen, O(5), in mannopyranose exhibits behaviour (g_{O5}) that is intermediate between hydrophobic and hydrophilic. The first peak is shifted out to 3.1–3.3 Å and is substantially smaller. Indeed, the height of less than one seems to indicate a local density of water below that of the bulk. There is also a very broad second peak centered at about 4.5 Å. This behaviour is best understood in terms of shielding effects. We have already noted that the methanolic oxygen will interfere with the hydration structure around O(5). O(5) is also well protected by the ring. In particular, O(5) will fall within the expected hydration 'sphere' of both C(1) and C(5). Thus there will be little space available for water molecules to approach O(5). To confirm this the g_{OMe} for methyl-α-D-mannopyranose is also depicted in Fig. 2; O(1) in this molecule is the etheric link between the methyl and monosaccharide groups, and so should be shielded in a similar way to O(5) in mannopyranose. The similarity in the two rdfs g_{OMe} and g_{O5} is clear, with the first peak at 3.1–3.3 Å diminished almost to the status of a shoulder and with a height of considerably less than 1. The second peak in g_{OMe} is more pronounced than that in g_{O5}, presumably because it has no neighbouring CH_2OH group.

The distribution of solute around various monosaccharide carbon atoms is depicted in Fig. 3. For the ring carbons, C(1) and C(5) in mannopyranose, (g_{C1} and g_{C5}) there is virtually no structure apart from the exclusion of solvent from their own volumes; the shift of the rdf to larger distances in C(5) is due to the CH_2OH substituent on this group. The pendant methyl groups, g_{OMe} in methyl-α-D-pyranoside and g_{Me} in 1-methyl-1-deoxy-α-D-mannopyranose both show hydrophobic behaviour as described above in connection with Fig. 2. It is interesting to note that g_{C6} for mannopyranose, the CH_2OH carbon, shows exactly the same solvent structure as these two methyl carbons, even though strong hydrogen bonding was found for O(6). Thus the structuring effect of the hydroxyl group is not apparent to the associated carbon. Indeed there is very little difference between these four curves, showing that the water distribution around the ring carbons is very similar to that found around the acyclic methyl groups, though g_{C5} is different and characteristic of a carbon atom with four non-hydrogen constituents. In contrast, the well-

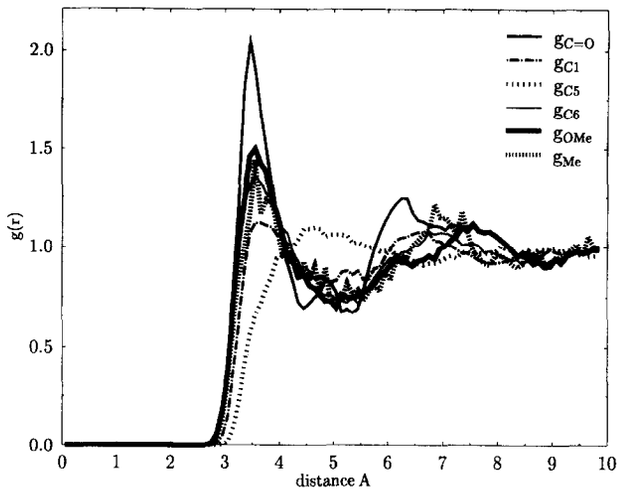

Fig. 3. Typical radial distribution curves $g(r)$ for C(1) in glucono-1,5-lactone, $g_{C=O}(r)$; the ring C(1) in α-D-mannopyranose, $g_{C1}(r)$; the ring carbon atom C(5) in α-D-mannopyranose $g_{O5}(r)$; the acyclic carbon C(6) in α-D-mannopyranose $g_{C6}(r)$; the carbon atom of the methyl group in methyl-α-D-mannopyranose, $g_{OMe}(r)$ and the carbon atom of the methyl group replacing the O(1) hydroxide in 1-methyl-1-deoxy-α-D-mannopyranose, $g_{Me}(r)$; from dynamics runs on the appropriate compounds.

defined structure in $g_{C=O}$ is a direct consequence of the strong solvent-structuring power already noted for the associated O(1) atom. It has been conjectured in other contexts that these variations in the ability of different groups to induce solvent structure may be implicated in optimizing biological activity (Fidler *et al.*, 1993). The slightly shorter than expected C...O distances are in keeping with those reported previously from crystal structures of sugars (Steiner & Saenger, 1992) and can be explained by the fact that the strong O–H...O hydrogen bonds will draw the water molecules closer to the C–H groups in the solute than the sum of van der Waals radii.

The $g(r)$ curves for two different hydrogen atoms are shown in Fig. 4. g_{CH} shows the rdf for the hydrogen bonded directly to C(1), while g_{OH} shows the rdf for the

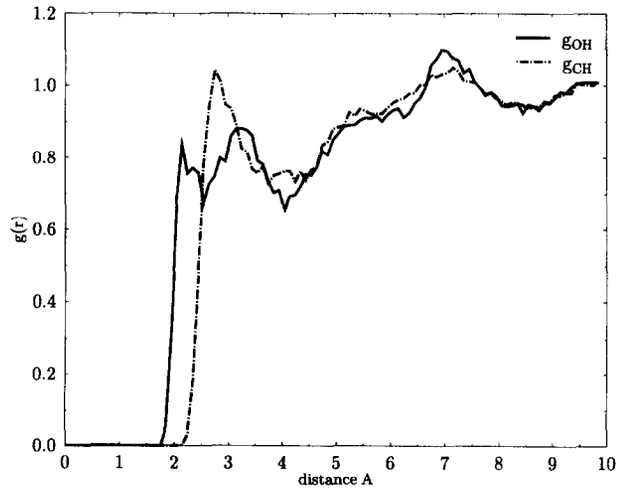

Fig. 4. Typical radial distribution curves $g(r)$ for hydrogen atoms bonded to carbon, $g_{CH}(r)$, and to oxygen, $g_{OH}(r)$, calculated from a dynamics run on α-D-mannopyranose.

hydrogen bonded to O(1). g_{OH} shows a sharp peak at *ca.* 2.1 Å which is characteristic of the first hydrogen bonding shell of oxygen atoms. The first peak in g_{CH} is at a slightly larger distance and is significantly weaker. The g_{OH} curves for the hydroxyls can be used to evaluate whether hydroxyl groups in the carbohydrates are acting as donor or acceptors in the hydrogen bonds that are formed.

In summary then, the radial distribution functions shown in Figs 2–4 clearly demonstrate that radial distribution functions are extremely valuable in indicating the arrangement of solvent molecules around specific atoms in the carbohydrate and in providing information about the hydrophobic and hydrophilic areas of the solute.[1]

α-D-mannopyranose and β-D-mannopyranose

The previous section provides a useful background against which to discuss the molecular dynamics results for α-D-mannopyranose and β-D-mannopyranose in detail. As shown above the rdfs can be used to distinguish between different types of atom, but they also provide information about the different water-structuring properties of similar atoms, for example the various hydroxide groups in the two structures.

Radial distribution functions

Selected radial distribution functions for α-D-mannopyranose are shown in Figs 5 and 7, and β-D-manno-

[1]Another function that provides information about the hydrogen bond pattern around the solute is the angular distribution function (adf) which arises because the hydrogen bond introduces an angular dependence that should give rise to orientational correlations between solute and solvent. The adf usually considered is the integrally normalized probability for each water molecule being orientated such that it makes an angle Θ between its OH bond vectors and the vector from the water oxygen to the carbohydrate atom. This function is calculated for those molecules within 3.5 Å of the carbohydrate atom, i.e. the distance that marks the first minimum in the pair distribution function for that atom. However, reliable angular distribution functions are difficult to obtain. In our studies we have not always found a pattern that fits with the ideal distribution function for hydrophobic and/or hydrophilic groups. Brady (1989) has also found such variations but has obtained sharply patterned curves by taking a short segment of the dynamics run and analysing that only, justifying this procedure by stating that 'only during the final few picoseconds of the simulation, ... did the adjacent water molecules reorient to the more 'ideal' hydrogen-bonding pattern'. This seems to imply that one needs to start with a minimized structure to get the 'correct' angular distributions; a process we have not attempted. It also seems to imply that there is not much flexibility in the carbohydrate once the simulation starts. A more likely conclusion, however, is that the 'ideal' pattern is less typical than one expects, and there are substantial fluctuations away from such ideal arrangements that may last for tens of picoseconds, in which case very long simulations would be needed to obtain reliable adfs. For that reason we have not shown our angular distribution functions here but have relied more on the rdfs to obtain the nature of the hydrogen bond pattern around the various hydroxyls in the carbohydrates.

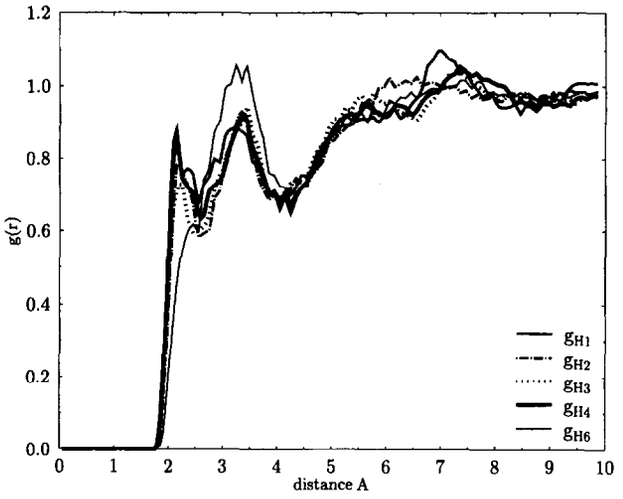

Fig. 5. Radial distribution functions $g_{Hn}(r)$ for water molecules around hydrogen atoms, H*n*, in hydroxyl groups in α-D-mannopyranose.

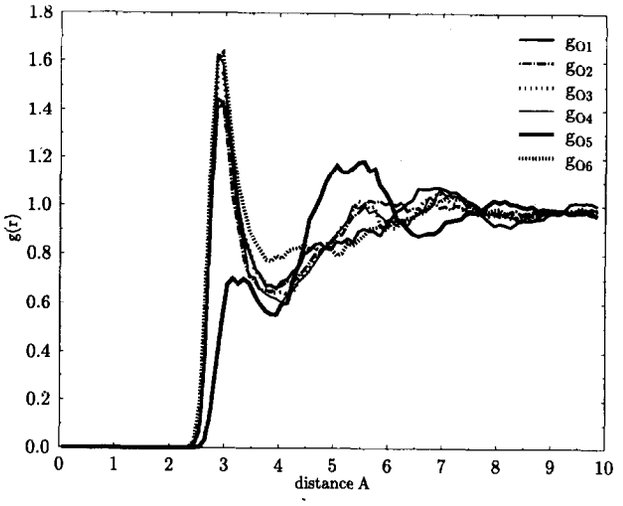

Fig. 6. Radial distribution functions $g_{On}(r)$ for water molecules around oxygen atoms, O*n*, in hydroxyl groups in α-D-mannopyranose. Note that g_{O2}, g_{O3} and g_{O4} overlap.

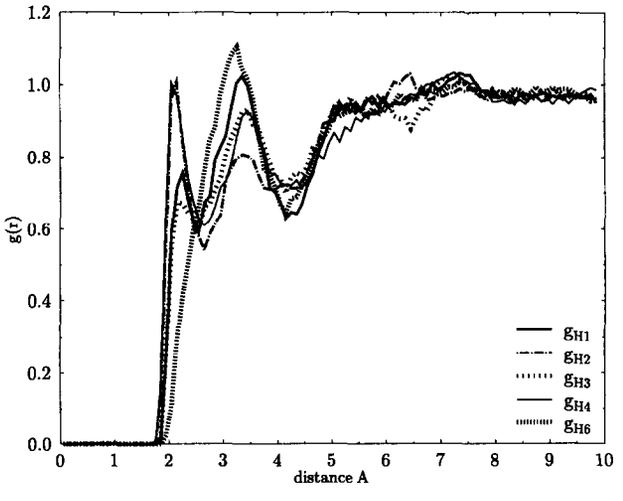

Fig. 7. Radial distribution functions $g_{Hn}(r)$ for water molecules around hydrogen atoms, H*n*, in hydroxyl groups in β-D-mannopyranose.

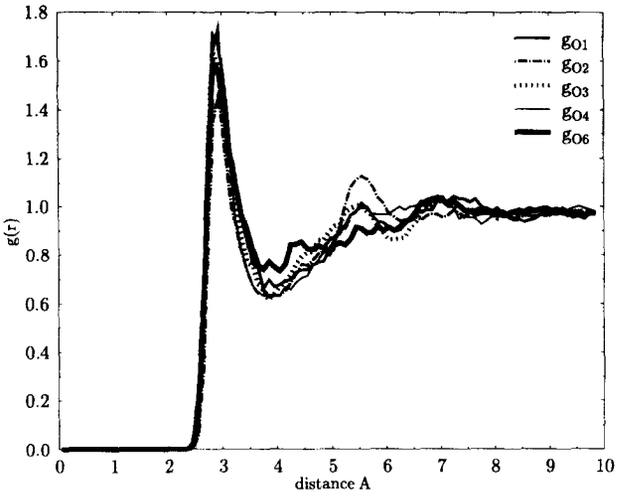

Fig. 8. Radial distribution functions $g_{On}(r)$ for water molecules around oxygen atoms, O*n*, in hydroxyl groups in β-D-mannopyranose.

pyranose in Figs 6 and 8. There are of course many rdfs that could be used to describe the arrangement of both oxygen and hydrogen atoms in the water molecules around either the oxygen or hydrogen atom in the hydroxyl group. In these figures we present the rdfs of water oxygen atoms around the hydroxyl hydrogen atoms (Figs 5 and 7) and the hydroxyl oxygen atoms (Figs 6 and 8) as this provides a good measure of the most significant solvation structure.

Figures 5 and 7 show the $g(r)$ curves for the hydrogen atoms in α-D-mannopyranose and β-D-mannopyranose. In both curves we can see the first peak for g_{H6} is at a far larger distance and is smaller than those for the other hydroxyl hydrogens. In α-D-mannopyranose, the initial peaks for the other four hydrogen atoms are very similar, but in β-D-mannopyranose the peaks in g_{H2} and g_{H4} are sharper and stronger than the others.

Figures 6 and 8 show the corresponding curves for the oxygen atoms in the two mannopyranoses. Here the differences are less striking than for the hydrogen atoms. All oxygen atoms exhibit sharp peaks at *ca.* 3.0 Å which is indicative of the first shell of water molecules as described above. In Fig. 7 we include the $g(r)$ curve for O(5) for comparison. As discussed previously this curve shows only a weak first shell at $r > 3.0$ Å but a much larger peak at *ca.* 5.0 Å. Despite the appearance of similarity there are variations in the peaks for the oxygen atoms that can be quantified and this is discussed below.

However, before attempting to correlate these differences in hydration with sweet-taste response it is important to be able to ensure that the differences in $g(r)$ are significant. For that reason we have repeated the calculations for both structures, but starting with a different solvent structure. In particular, the solute molecule was rotated by 90° before insertion into the water box, with subsequent deletion of different overlapping water molecules and relaxation of the resulting structure. The molecular dynamic runs were repeated and the rdfs recalculated. As a measure of the differences associated with the choice of initial configuration, each rdf was tabulated at 0.05 Å intervals from 0.0 Å to 10.0 Å and the values used to calculate the rms deviation between them. Using this measure the difference within each pair of analogous simulations was only *ca.* 0.02–0.03, which does indicate effective sampling of the set of solvent configurations that characterizes equilibrium. These values are much smaller than the rms difference of 0.09 between the α and β anomers, and confirms that the differences noted above are indeed significant. This difference is apparent from the appearance of the g_{O2} curve in Figs 6 and 8, specifically in the latter where there is a significant peak at *ca.* 5.5 Å.

Hydrogen bond numbers

In order to quantify the information from the rdfs it is convenient to introduce two additional measures: the coordination number of each atom, and the number of hydrogen bonds it participates in. The former is just a measure of the number of atoms or molecules found within the first solvation shell of a given solute atom, and this is readily calculated from the volume-weighted integral of the rdf. A working definition of the radius of the solvation shell is needed, and for this we have adopted the position of the first minimum in the rdf. From Figs 2–4 it is clear that the position of this first minimum is influenced by both the type of solute atom, and its environment. We have therefore confined our attention to the coordination number of the oxygen atoms, and defined the radius of the solvation shell from the rdf that shows the least environmental influence, $g_{C=O}$ in glucono-1,5-lactone (Fig. 2). This gives a radius of 3.5 Å.

A working definition is also needed for the hydrogen bond numbers, and in this case a simple distance criterion is insufficient as the orientation of the water molecules must also be appropriate for hydrogen bonding. A number of studies have been published which address this issue. Kroon *et al.* (1975) looked at the crystal structures of 45 polyalcohols and found the O...O distance in a hydrogen bond as being between 2.60 and 3.05 Å. They also found the most common O–H...O angle was ~160°. Sometime later Ceccarelli *et al.* (1981) used more accurate neutron diffraction data from 24 structures and obtained a mean H...O distance of 1.805(9) Å and a mean O–H...O angle of 167.1(8)°. However, the geometry of hydrogen bonds will depend on the electrostatic properties of the atoms involved (Umeyama & Morokuma, 1977); thus even small changes in the environment may produce significant alterations in the dimensions of the hydrogen bonds. For example, theoretical calculations suggest that the hemiacetal ('anomeric') oxygen atom in pyranoses is electron-deficient compared with the other oxygen atoms in the molecule (Tse & Newton, 1977). Thus one would expect this atom to be an exceptionally good proton donor in hydrogen bonds. This was confirmed by a survey of carbohydrate crystal structures, which showed that O–H...O bonds tended to be shorter than others in the pyranose (Newton, 1983). Further, all

these structural studies involve average or minimum energy structures; thus still more variation in the geometry of a hydrogen bond should arise from the thermal motion of the atoms involved.

In view of these factors, we have adopted a combination of distance and angle qualifications for the definition of a hydrogen bond (Beveridge *et al.*, 1983): a hydrogen bond is said to exist if the O...O separation is less than 3.5 Å, and the O–H...O angle is greater than 120°. Using this criterion, we have calculated, for each configuration in the trajectory file, the number of hydrogen bonds observed around each oxygen and hydrogen atom of the hydroxyl groups in α-D-mannopyranose and β-D-mannopyranose. The average number of hydrogen bonds for these atoms and the total for each hydroxyl were then averaged over all configurations in the trajectory and the results are shown in Table 1.

Sweet-taste response

The information provided in Table 1 and Figs 5–8 can be used to draw conclusions about the differing nature of the carbohydrate oxygen atoms. From the hydrogen bond 'counts' presented in the first part of Table 1, it can be seen that all oxygen atoms except for O(1) in both α-D-mannopyranose and β-D-mannopyranose act more often as an acceptor than a donor, which is consistent with the values found by Galema *et al.* (1994) in a hydrogen bond count from a similar molecular dynamics study of β-galactose; however, direct comparison of the numbers is impossible due to the different definition that was used for a hydrogen bond (i.e. O...H < 2.4 Å and O–H...O $> 145°$). In our work, it is apparent from Table 1 that in α-D-mannopyranose, O(3) and O(4) are far better acceptors than O(1) and O(2), and that H(3) stands out as a particularly poor donor. This suggests a likely assignment of O(4)–H, O(3) as the A–H, B glucophore. This is supported by the g_H curves (Fig. 5) which predict also that O(4) is the best donor hydroxyl. There have been many attempts to identify the A–H,B glucophore in different monosaccharides (e.g. methyl α-D-glucopyranoside (Lindley & Birch, 1975) and fructose (Woods *et al.*, 1987; Mathlouthi & Portmann, 1990)) and, while there is general agreement on O(3) for B, both O(2) and O(4) have been characterized as A. MEP (molecular electrostatic potential) calculations (Lichtenthaler & Immel, 1993) have shown that for fructose the O(3), O(4) region is hydrophilic and the O(1), O(2) region hydrophobic, which supports an assignment of O(4)–H as A–H. Our data are consistent with these findings. It is interesting that the numbers of O...O distances under 3.5 Å reported in Table 1, and calculated from the areas under the first peak of the rdfs of the oxygen atoms, are about twice as large as the number of hydrogen bonds observed. Clearly many of these short distances represent structures where neither the hydrogen atoms in the water molecules nor those in the carbohydrate are located between the two oxygen atoms.

Table 1. Average number of hydrogen bonds formed during the molecular dynamics simulation of α-D-mannopyranose and β-D-mannopyranose

	α-D-mannopyranose	β-D-mannopyranose
O(1)	0.747	0.834
O(2)	0.854	1.135
O(3)	0.989	0.891
O(4)	1.028	1.086
O(6)	1.214	1.137
H(1)	0.919	1.021
H(2)	0.764	0.743
H(3)	0.737	0.796
H(4)	0.824	0.986
H(6)	0.537	0.362
Total counts of hydrogen bonds compared to values (in brackets) obtained by calculating the areas under the first peak in the rdfs of the oxygen atoms up to 3.5 Å		
O(1) + H(1)	1.666(3.440)	1.855(3.385)
O(2) + H(2)	1.618(3.248)	1.878(4.029)
O(3) + H(3)	1.726(3.639)	1.688(3.820)
O(4) + H(4)	1.853(3.574)	2.072(3.427)
O(6) + H(6)	1.751(3.944)	1.500(3.950)

Both the rdfs and the hydrogen-bond numbers for α-D-mannopyranose indicate that O(3), O(4) and O(6) are more involved in hydrogen bond formation than are O(1) and O(2). This is consistent with the MEPs (described above for fructose) which show that the O(3), O(4), O(6) side of the molecule is more hydrophilic than the O(1), O(2) side. Indeed it has been argued (Lichtenthaler & Immel, 1993) that the hydrophobic end of the fructose molecule binds to the corresponding hydrophobic site in the receptor and is a crucial part of the sweet response.

Having designated the AH–B glucophore, we can then locate the XH group as O(1)–H. In this case the dimensions of the A,B,X triangle are relatively constant during the molecular dynamics run, although the positions of the hydrogen atoms on A and X vary significantly. Generally though, it is important to take into account the significant flexibility of carbohydrates in any calculation of structure/activity relationships. In this case the distances between the non-hydrogen atoms in the carbohydrate do not change very much during the course of the simulation and the major changes are found in the hydrogen positions, but in other sweeteners there may be a lower barrier to rotation around some of the bonds so that the positions of non-hydrogen atoms could move significantly. Of course this very flexibility does allow the carbohydrate to change its conformation to fit into the receptor site if necessary.

In contrast with the sweet-tasting α anomer, β-D-mannopyranose is bitter. As is apparent from Table 1, the hydrogen bond counts from the molecular dynamics results are significantly different. Particularly striking is the increase in the number of acceptor hydrogen bonds formed by O(2) and to a lesser extent O(1). At the same time, the ability of O(1) to form acceptor hydrogen bonds is also increased, while that of the other atoms remains

relatively unchanged. This increase in the water population around O(1) and O(2) is concomitant with a significant decrease in the water population around O(3). Clearly for β-D-mannopyranose it is not possible to assign hydrophilic and hyrophobic ends to the molecule as in the α-analogue and this may account, following the hydrophobic theory of Lichtenthaler & Immel (1993), for the lack of sweet taste in the β form.

Although our data for α-D-mannopyranose lend strong credence to the assignment of O(4)–H, O(3),O(1) as the AH,B,X triangle, this assignment cannot be called unequivocal. Clearly, though, this triangle cannot be present in the β-D-mannopyranose because of the different position of O(1) and this may account for the difference in taste properties. However, a concomitant reason may well be the spectacular differences in the hydration structure around O(1) and O(2) between the α and β forms which precludes the existence of the hydrophobic side to the molecule that is considered essential by many current theories.

CONCLUSIONS

We have shown that the calculation of rdfs from molecular dynamics simulations is a very useful general tool for establishing the differences in the water structuring properties of the various groups in carbohydrates. In our work on α-D-mannopyranose and β-D-mannopyranose we have found very significant differences between the arrangement of water molecules around the specific oxygen atoms, particularly O(2), which have been correlated with the taste properties of these molecules.

ACKNOWLEDGEMENTS

We thank the EC (AIR program; PL 94–2107) and the UK BBSRC for support.

REFERENCES

Berendsen, H. J. C., Grigera, J. G. & Straatsma, T. P. (1987). The missing term in effective pair potentials, *J. Phys. Chem.*, **91**, 6269–71.

Berendsen, H. J. C., Postma, P. M., von Gunsteren, W. F. & Hermans, J. (1981). *Intermolecular Forces*, ed. B. Pullman. Reidel, Dordrecht, Holland, 331 pp.

Beveridge, D. L., Mezei, M., Mehrotra, P. K., Marchese, F. T. & Ravi-Shanker, G. (1983). Monte-Carlo computer simulation studies of the equilibrium properties and structure of liquid water. *Adv. Chem. Ser.*, **204**, 297–351.

Birch, G. G., Karim, R., Chavez, A. L. & Morini, G. (1993). Sweetness, structure and specific volume. In *Sweet-Taste Chemoreception*, eds M. Mathlouthi, J. A. Kanters & G. G. Birch. Elsevier Applied Science, London, pp. 129–39.

Brady, J. W. (1989). Molecular dynamics simulations of α-D-glucose in aqueous solution. *J. Am. Chem. Soc.*, **111**, 5155–65.

Brooks, B. R., Bruccoleri, R. E., Olafson, B. D., States, D. J., Suaminathan, S. & Karplus, M. (1983). CHARMm — a program for macromolecular energy, minimization, and dynamics calculations. *J. Comput. Chem.*, **4**, 187.

Ceccarelli, C., Jeffrey, G. A. & Taylor, R. (1981). A survey of O–H...O hydrogen bond geometries determined by neutron diffraction. *J. Mol. Struct*, **70**, 255–71.

Cieplak, P. & Kollman, P. (1991). On the use of electrostatic potential derived charges in molecular mechanics force fields. The relative solvation free energy of *cis* and *trans*-*N*-methyl-acetamide. *J. Comp. Chem.*, **12**, 1232–6.

Fidler, J., Rodger, P. M. & Rodger, A. (1993). Chiral solvent structure around chiral molecules: experimental and theoretical study. *J. Chem. Soc. Perkin Trans.*, **2**, 235.

Galema, S. A., Howard, E., Engberts, J. B. F. N. & Grigera, J. R. (1994). The effect of stereochemistry upon carbohydrate hydration, A molecular dynamics simulation of β-D-galactopyranose and (α,β)-D-talopyranose. *Carbo. Res.*, **265**, 215–25.

Grootenhuis, P. D. J. & Haasnoot, C. A. G. (1993). A CHARMm based force field for carbohydrates using the Cheat approach. Carbohydrate hydroxyl groups represented by extended atoms. *Mol. Sim.*, **10**, 75–95.

Ha, S., Gao, J., Tidor, B., Brady, J. W. & Karplus, M. (1991). Solvent effect on the anomeric equilibrium in D-glucose: a free energy simulation analysis. *J. Am. Chem. Soc.*, **113**, 1553–7.

Jorgensen, W. L., Chandrasekhar, J., Madura, J. D., Impney, R. W. & Klein, M. L. (1983). Comparison of simple potential functions for simulating liquid water. *J. Chem. Phys.*, **79**, 926–35.

Kier, L. B. (1972). Molecular theory of sweet taste. *J. Pharm. Sci.*, **61**, 1394–7.

Kroon, J., Kanters, J. A., van Duijneveldt-van de Rijdt, J. G. C. M., van Duijneveldt, F. B. & Vliegenthart, J. A. (1975). O–H...O hydrogen bonds in molecular crystals. A statistical and quantum chemical analysis. *J. Mol. Struct.*, **24**, 109–29.

Langchambon, F., Averal, D. & Newman, A. (1976). Structure crystalline de l'α-D-mannopyranose, *Acta Cryst*, **B32**, 1822.

Lichtenthaler, F. W. & Immel, S. (1993). Sucrose, sucralose and fructose: correlations between hydrophobicity potential profiles and AH–B–X assignments. In *Sweet-Taste Chemoreception*, eds M. Mathlouthi, J. A. Kanters & G. G. Birch. Elsevier Applied Science, London, UK, pp. 21–53.

Lindley, M. G. & Birch, G. G. (1975). Structural functions of taste in the sugar series. *J. Sci. Food Agric.*, **26**, 117.

Madsen, L. J., Ha, S. N., Tran, V. H. & Brady, J. W., (1990), Molecular dynamics simulations of carbohydrates and their solvation. In *Computer Modeling of Carbohydrate Molecules*, eds A. D. French & J. W. Brady. American Chemical Society, Washington, D.C., USA, pp. 69–90.

Mathlouthi, M. & Portmann, M. O. (1990). Hydrogen-bonding and the sweet taste mechanism. *J. Mol. Struct.*, **237**, 327.

Newton, M. D. (1983). Theoretical aspects of the OH...O hydrogen-bond and its role in structural and kinetic phenomena. *Acta Crystallogr., Sect. B*, **B39**, 104–13.

Pautet, F. & Nofre, C. (1978). Correlation of chemical structure and taste in the cyclamate series and the steric nature of the chemoreceptor site. *Zeitsch. Lebensmn. Unters-und-Forsch.*, **166**, 167–70.

Quanta/CHARMm (1994). Molecular Simulations Inc., Burlington, MA, CHARMm version 23.

Shallenberger, R. S. (1963). Hydrogen bonding and the varying sweetness of sugars. *J. Food Sci.*, **28**, 584–9.

Shallenberger, R. S. & Acree, T. E. (1967). Molecular theory of sweet taste. *Nature*, **216**, 480–2.

Shallenberger, R. S., Acree, T. E. & Lee, C. K. (1969). Sweet taste of D- and L-sugars and amino acids and the steric nature of their chemo-receptor site. *Nature*, **221**, 555–6.

Steiner, T. & Saenger, W. (1992). Geometry of C–H...O hydrogen bonds in carbohydrate crystal structures.

Analysis of neutron diffraction data. *J. Am. Chem. Soc.*, **114**, 10146–54.

Tinti, J. M. & Nofre, C. (1990). Design of sweeteners. In *Sweeteners: Discovery, Molecular Design and Chemoreception*, eds D. E. Walters, F. T. Orthoefer & G. E. Dubois. American Chemical Society Symposium Series 450, pp. 88–99.

Toukan, K. & Rahman, A. (1985). Molecular dynamics study of atomic motions in water, *Phys. Rev. B*, **31**, 2643.

Tse, Y.-C. & Newton, M. D. (1977). Theoretical observations on the structural consequences of cooperativity in H...O hydrogen bonding. *J. Am. Chem. Soc.*, **99**, 611–3.

Umeyama, H. & Morokuma, K. (1977). The origin of hydrogen bonding—an energy decomposition study. *J. Am. Chem. Soc.*, **99**, 1316–32.

van der Heijden, A., van der Wel, H. & Peer, H. G. (1985). Structure-activity relationships in sweeteners. I. Nitroanilines, sulphamates, oximes, isocoumarins and dipeptides. *Chem. Senses*, **10**, 57–72.

van Eijck, B. P., Kroon-Batenburg, L. M. J. & Kroon, J. (1990). Hydrogen-bond geometry around sugar molecules: comparison of crystal statistics with simulated aqueous solutions. *J. Mol. Struct.*, **237**, 315–25.

van Gunsteren, W. F. & Berendsen, H. J. C. (1977). Algorithms for macromolecular dynamics and constraint dynamics. *Mol. Phys.*, **34**, 1311–27.

Verlet, L. (1967). Computer 'experiments' on classical fluids. I. Thermodynamical properties of Lennard–Jones molecules. *Phys. Res.*, **159**, 98.

Withers, S. G., Street, I. P. & Rettig, S. J. (1986). The preferred conformation of 2-fluoro-2-deoxy β-D-mannopyranose fluoride. An X-ray crystallographic and two-dimensional nuclear magnetic resonance study. *Can. J. Chem.*, **64**, 232.

Woods, R. J., Smith, V. H. Jr., Szarek, W. A. & Farazdel, A. (1987). *Ab-initio* lcao-mo calculations on α-D-glucopyranose, β-D-fructopyranose and their thiopyranoid ring analogs—application to a theory of sweetness. *J. Chem. Soc. Chem. Commun.*, 937–9.